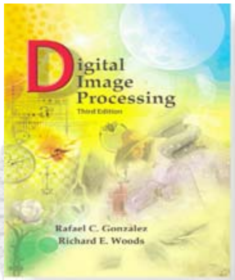

Lecture #19

- Shading and texture analysis using morphology
- Gray scale reconstruction
- Basic image segmentation: edges v. regions
- Point and line locators, edge types and noise
- Edge operators: LoG, DoG, Canny

Gray Scale Morphology

original

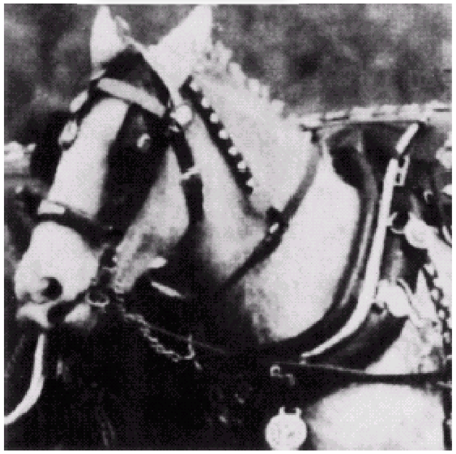

"top-hat"

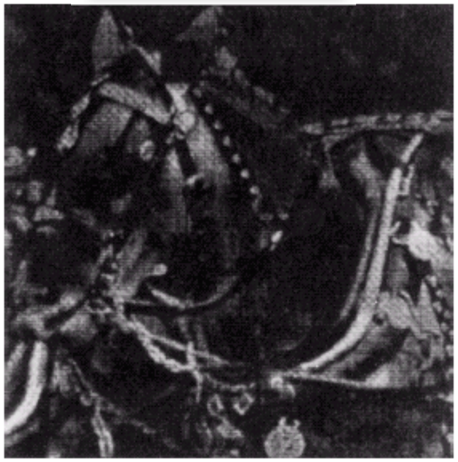

$$h = f - (f \circ b)$$

A top-hat transformation subtracts an opening from the image.

FIGURE 9.34 Result of performing a top-hat transformation on the image of Fig. 9.29(a). (Courtesy of Mr. A. Morris, Leica Cambridge, Ltd.)

Enhances detail in the presence of shading

Gray-Scale Morphology

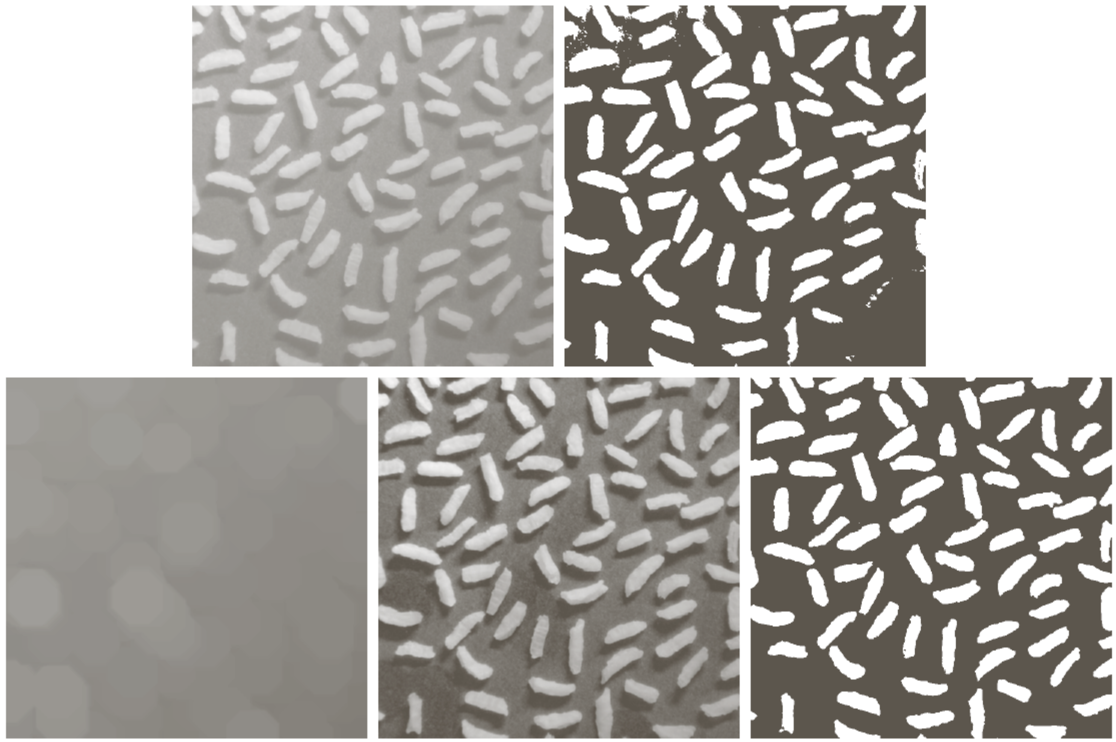

a b
c d e

FIGURE 9.40 Using the top-hat transformation for *shading correction*. (a) Original image of size 600 × 600 pixels. (b) Thresholded image. (c) Image opened using a disk SE of radius 40. (d) Top-hat transformation (the image minus its opening). (e) Thresholded top-hat image.

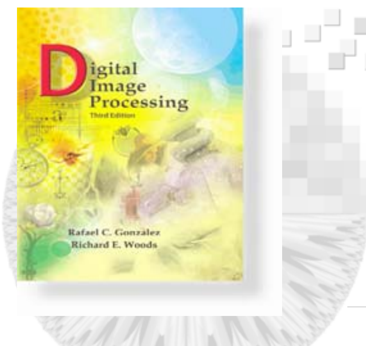

Chapter 9
Morphological Image Processing

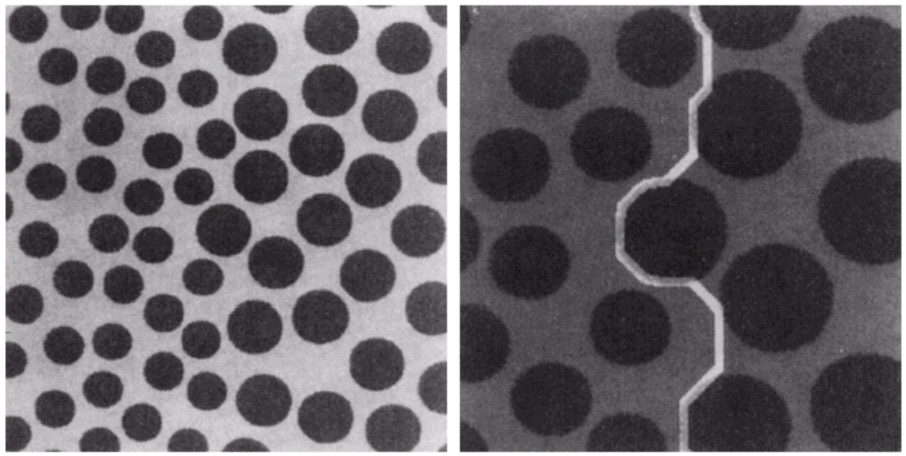

a b

FIGURE 9.35 (a) Original image. (b) Image showing boundary between regions of different texture. (Courtesy of Mr. A. Morris, Leica Cambridge, Ltd.)

FIGURE 9.42 Differences in surface area as a function of SE disk radius, r. The two peaks are indicative of two dominant particle sizes in the image.

Gray-Scale Morphology

<u>Algorithm for locating texture boundaries</u>

1. Repeatedly close the input image with a SE smaller than the large circles. This will eventually remove all the smaller objects.
2. Now do a single opening with a SE larger than the separation between right hand circles
3. Use a morphological gradient to compute the boundary

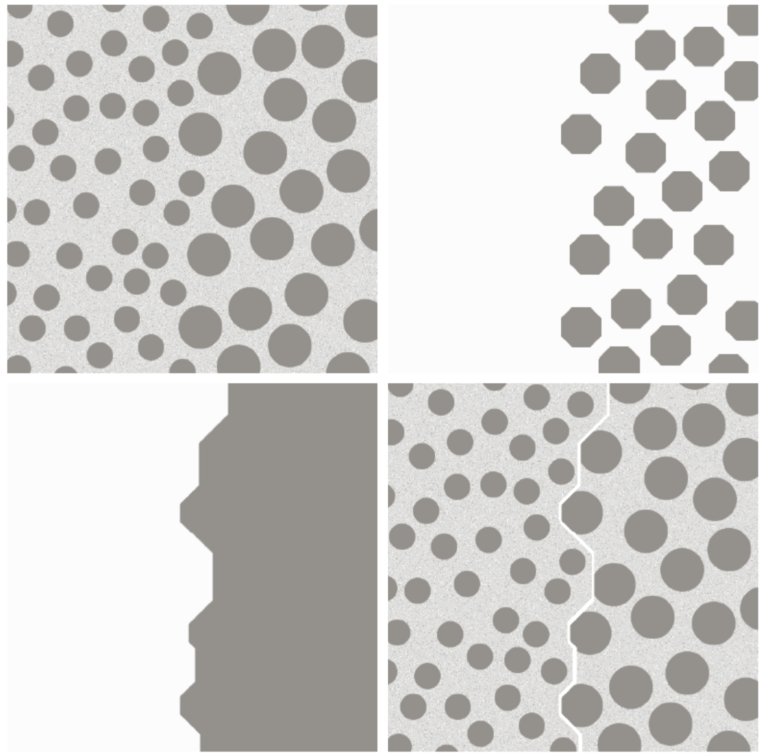

a b
c d

FIGURE 9.43 Textural segmentation. (a) A 600 × 600 image consisting of two types of blobs. (b) Image with small blobs removed by closing (a). (c) Image with light patches between large blobs removed by opening (b). (d) Original image with boundary between the two regions in (c) superimposed. The boundary was obtained using a morphological gradient operation.

Gray-Scale Morphology

Smooth to eliminate wood grain

Open with r=10 disk

Open with r=20 disk

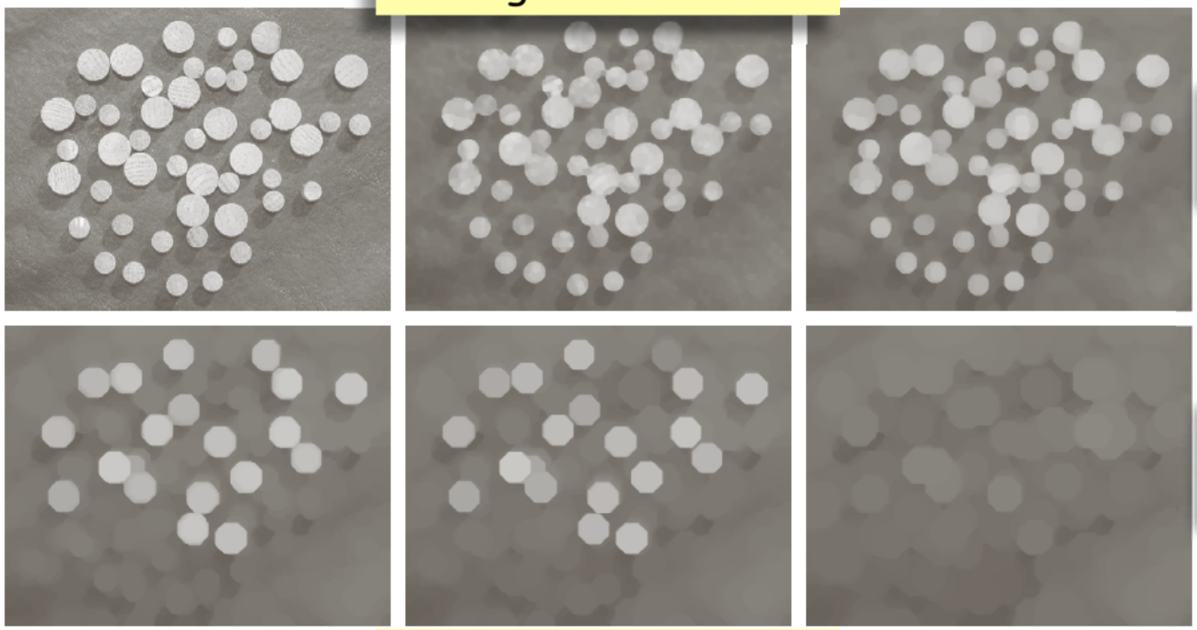

Open with r=25 disk

Open with r=30 disk

a b c
d e f

FIGURE 9.41 (a) 531 × 675 image of wood dowels. (b) Smoothed image. (c)–(f) Openings of (b) with disks of radii equal to 10, 20, 25, and 30 pixels, respectively. (Original image courtesy of Dr. Steve Eddins, The MathWorks, Inc.)

Summing the surface area (light intensity) and subtracting to determine the change as a function of r gives the particle size distribution

Gray-Scale Morphology

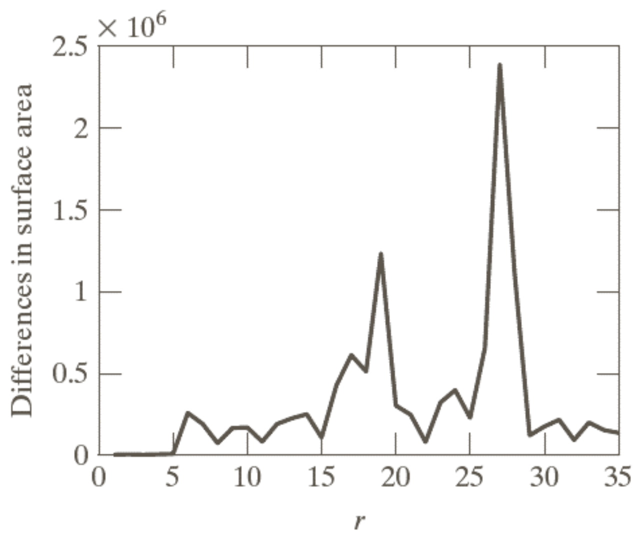

FIGURE 9.42 Differences in surface area as a function of SE disk radius, r. The two peaks are indicative of two dominant particle sizes in the image.

This shows that the image is basically composed of images of r=19 and r=27 particles

Gray Scale Morphology

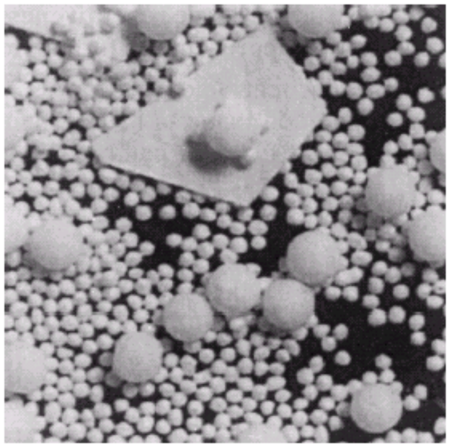


a b

FIGURE 9.36 (a) Original image consisting of overlapping particles; (b) size distribution. (Courtesy of Mr. A. Morris, Leica Cambridge, Ltd.)

<u>Granulometry — how to determine size distributions</u>

1. Open with structuring elements which increase in size with each iteration
2. Compute differences between original and each opening
3. Normalize these differences to give the size distribution

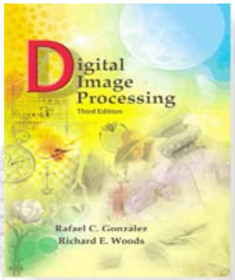

Original image

FIGURE 9.44 (a) Original image of size 1134 × 1360 pix pening by reconstruction of (a) using a horizontal line 71 pixels long in the erosion. (c) Opening of (a) using the same line. (d) Top-hat by reconstruction. (e) Top-hat. (f) Opening by reconstruction of (d) using a horizontal line 11 pixels long. (g) Dilation of (f) using a horizontal line 21 pixels long. (h) Minimum of (d) and (g). (i) Final reconstruction result. (Images courtesy of Dr. Steve Eddins, The MathWorks, Inc.)

This illustrates morphological reconstructio n to eliminate vertical and horizontal lines and shadows in an image.

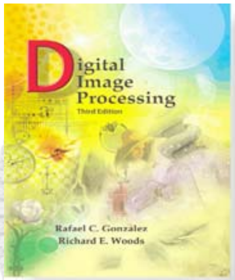

Chap. 10 Image Segmentation

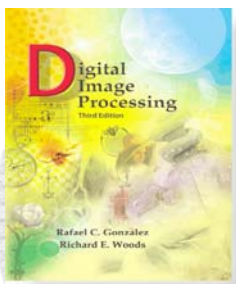

Image Segmentation

- Segmentation partitions image R into subregions R_1, R_2, …, R_n such that:
  - $R_1 \cup R_2 \cup \ldots \cup R_n = R$
  - Each R_i is a connected set
  - $R_i \cap R_j = 0$ for all i,j where $i \neq j$
  - Q(Ri)=TRUE for every i
  - $Q(R_i \cup R_j)$=FALSE for any two adjacent regions

Image Segmentation

Original images

Edge-based segmentation

Region-based segmentation

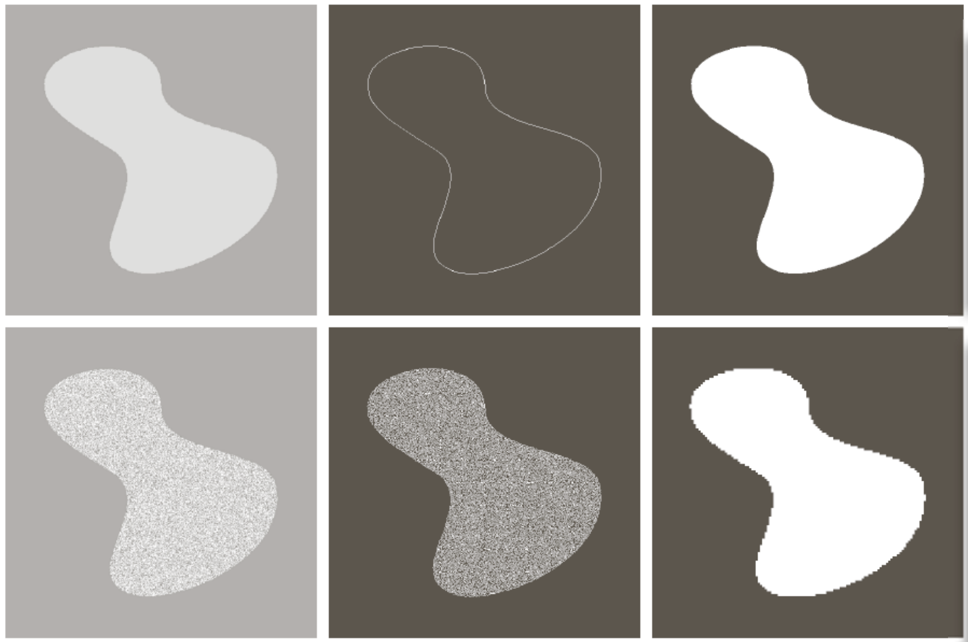

Segmented image. R_i are orthogonal and have different intensity.

Segmented image based upon standard deviation of the intensity in 4x4 regions

Boundaries obtained from derivatives or similar techniques

a b c
d e f

FIGURE 10.1 (a) Image containing a region of constant intensity. (b) Image showing the boundary of the inner region, obtained from intensity discontinuities. (c) Result of segmenting the image into two regions. (d) Image containing a textured region. (e) Result of edge computations. Note the large number of small edges that are connected to the original boundary, making it difficult to find a unique boundary using only edge information. (f) Result of segmentation based on region properties.

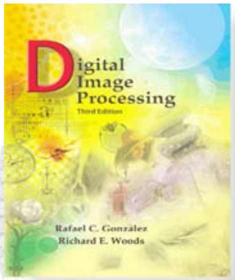

Line Detection

Edge based segmentation requires finding good edges — typically using a first or second derivative spatial operator.

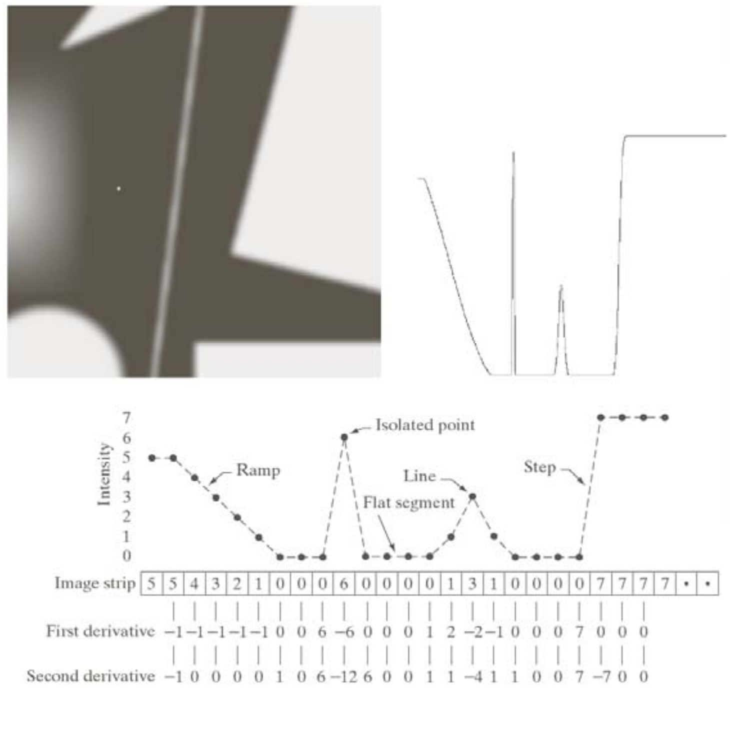

FIGURE 10.2 (a) Image. (b) Horizontal intensity profile through the center of the image, including the isolated noise point. (c) Simplified profile (the points are joined by dashes for clarity). The image strip corresponds to the intensity profile, and the numbers in the boxes are the intensity values of the dots shown in the profile. The derivatives were obtained using Eqs. (10.2-1) and (10.2-2).

There are multiple types of edges such as ramp and step giving different responses.

First derivative operators typically give thicker edge responses; second derivative operators respond to finer detail, including noise

Second derivates produce a double edge response for ramp and step edges

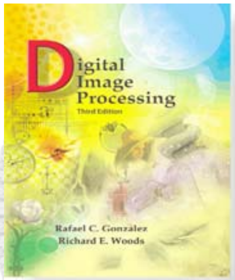

Line Detection

w_1	w_2	w_3
w_4	w_5	w_6
w_7	w_8	w_9

FIGURE 10.3 A general 3×3 spatial filter mask.

While we typically regarded a mask such as the 3x3 shown above as a spatial operator it can also be thought of as a correlation mask.

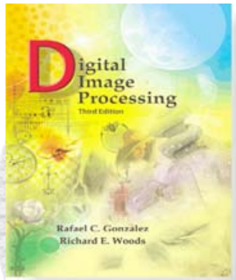

Line (and point) Detection

Single black pixel we want to find

1	1	1
1	−8	1
1	1	1

Regard this as a correlation mask for a black pixel, i.e., a point locator

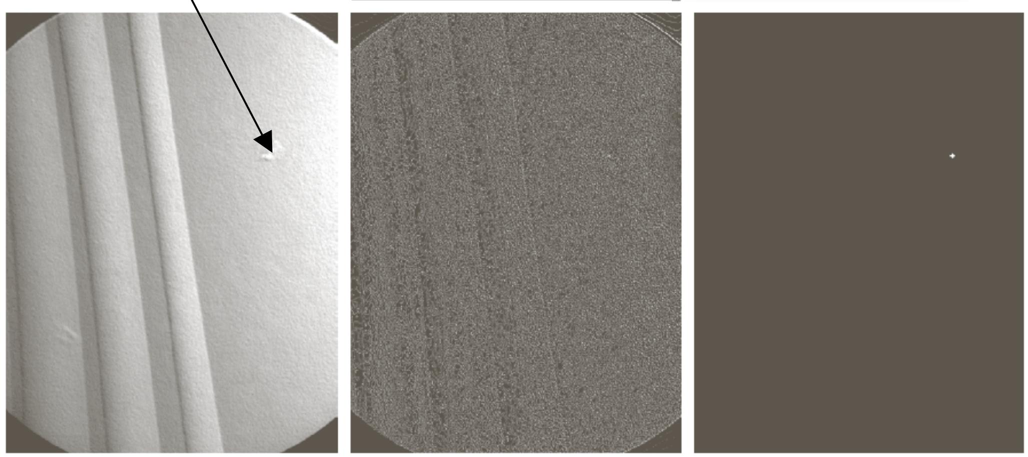

a
b c d

FIGURE 10.4 (a) Point detection (Laplacian) mask. (b) X-ray image of turbine blade with a porosity. The porosity contains a single black pixel. (c) Result of convolving the mask with the image. (d) Result of using Eq. (10.2-8) showing a single point (the point was enlarged to make it easier to see). (Original image courtesy of X-TEK Systems, Ltd.)

$$R = \sum_{i=1}^{9} w_i z_i$$

Response R to correlation mask

Threshold at T=90 of max pixel intensity

Line Detection

Original image

Laplacian processed image. Intensity transformed so 50% gray is zero. Double line effect is clearly visible.

Absolute value of the Laplacian gives wide lines

Using only positive values of the Laplacian gives narrower lines.

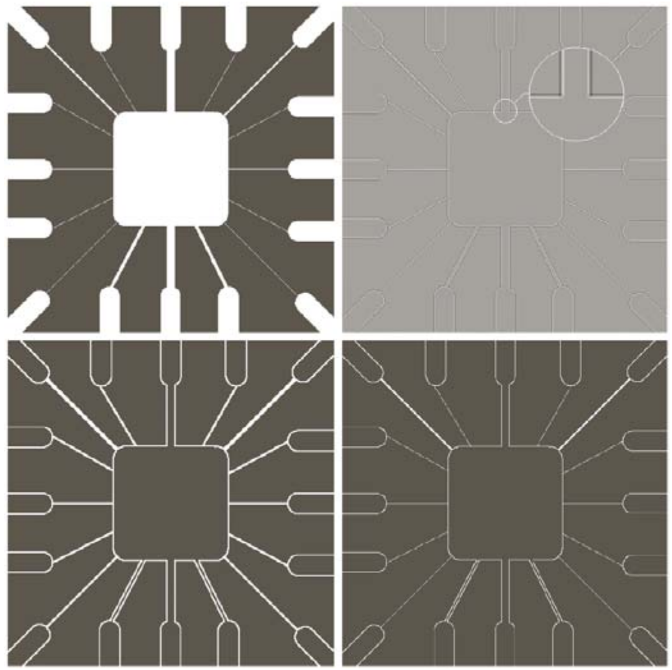

a b
c d

FIGURE 10.5
(a) Original image.
(b) Laplacian image; the magnified section shows the positive/negative double-line effect characteristic of the Laplacian.
(c) Absolute value of the Laplacian.
(d) Positive values of the Laplacian.

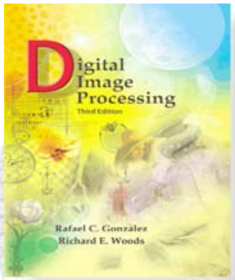

Line Detection

−1	−1	−1
2	2	2
−1	−1	−1

Horizontal

2	−1	−1
−1	2	−1
−1	−1	2

+45°

−1	2	−1
−1	2	−1
−1	2	−1

Vertical

−1	−1	2
−1	2	−1
2	−1	−1

−45°

FIGURE 10.6 Line detection masks. Angles are with respect to the axis system in Fig. 2.18(b).

These can be regarded as line detector masks for lines with specific orientations.

Line Detection

Original image

Response using +45° line detector

Zoom of top left response

Zoom of bottom right response

Response with all negative values set to zero

Select only maximum values from (e)

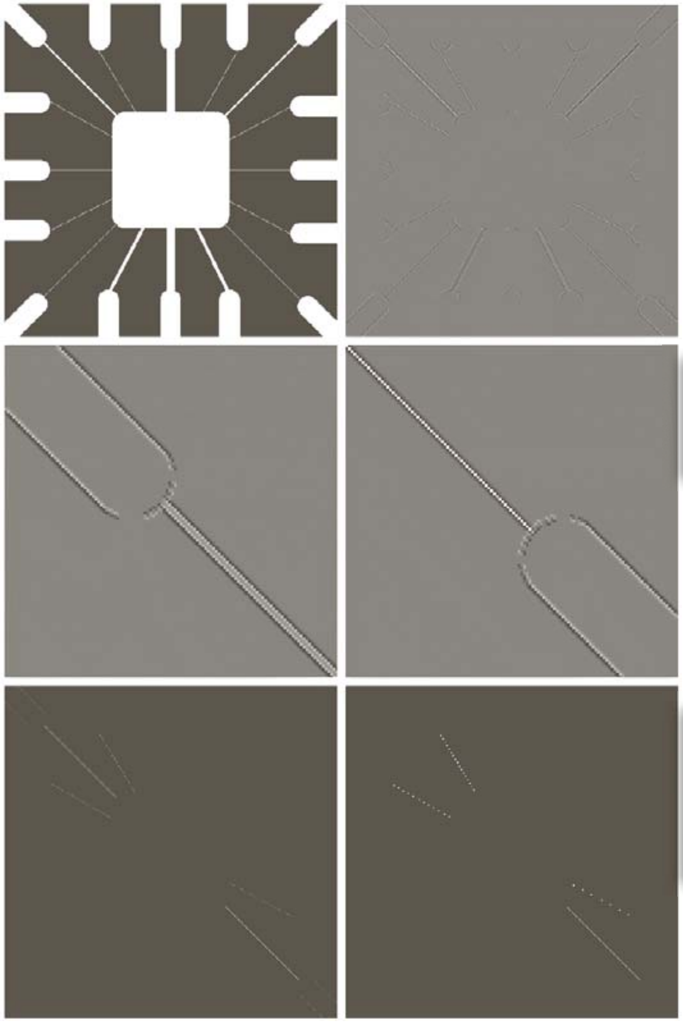

a b
c d
e f

FIGURE 10.7 (a) Image of a wire-bond template. (b) Result of processing with the +45° line detector mask in Fig. 10.6. (c) Zoomed view of the top left region of (b). (d) Zoomed view of the bottom right region of (b). (e) The image in (b) with all negative values set to zero. (f) All points (in white) whose values satisfied the condition $g \geq T$, where g is the image in (e). (The points in (f) were enlarged to make them easier to see.)

Line Detection

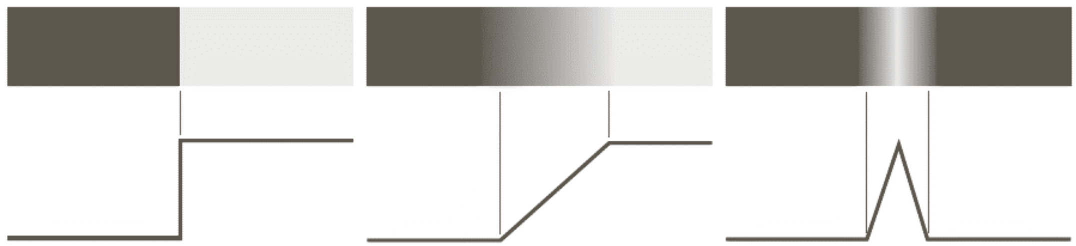

Step edge and its intensity profile.

Ramp edge and its intensity profile.

Roof edge and its intensity profile.

a b c

FIGURE 10.8 From left to right, models (ideal representations) of a step, a ramp, and a roof edge, and their corresponding intensity profiles.

Line Detection

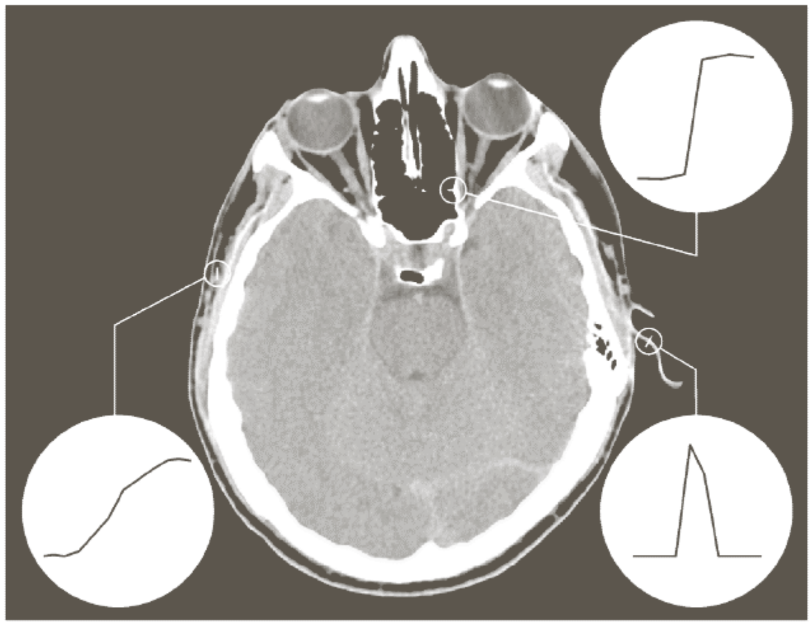

FIGURE 10.9 A 1508 × 1970 image showing (zoomed) actual ramp (bottom, left), step (top, right), and roof edge profiles. The profiles are from dark to light, in the areas indicated by the short line segments shown in the small circles. The ramp and "step" profiles span 9 pixels and 2 pixels, respectively. The base of the roof edge is 3 pixels. (Original image courtesy of Dr. David R. Pickens, Vanderbilt University.)

Real intensity image showing multiple types of edges

Line Detection

Observations:
1. Magnitude of the first derivative can be used to detect the presence of an edge at a point
2. Sign of second derivative indicates which side of the edge the pixel is on
3. Zero crossings of the second derivative can be used to locate the centers of thick edges

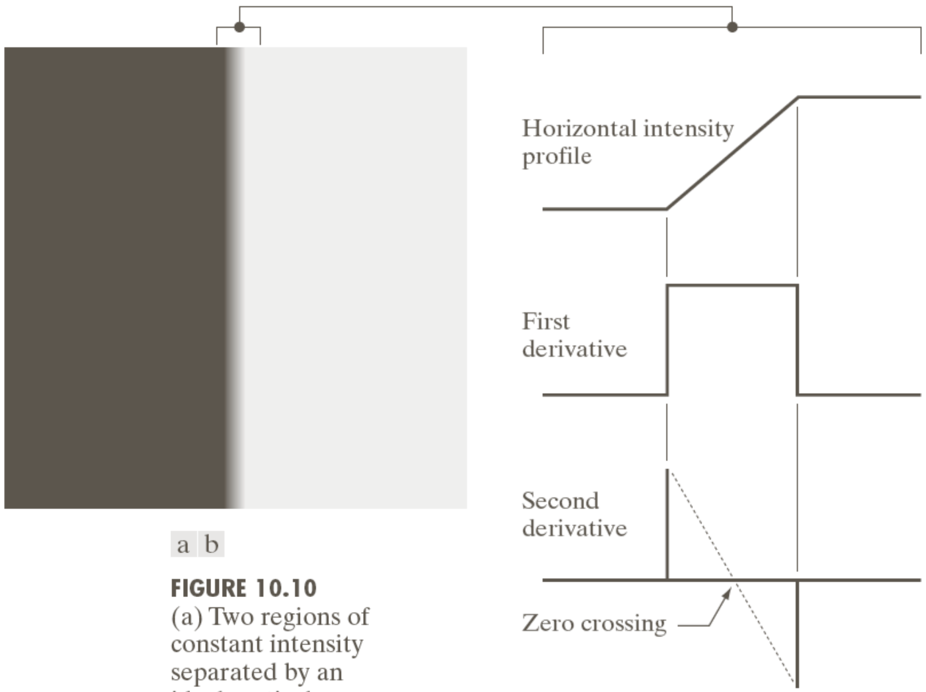

a b

FIGURE 10.10 (a) Two regions of constant intensity separated by an ideal vertical ramp edge. (b) Detail near the edge, showing a horizontal intensity profile, together with its first and second derivatives.

Line Detection

First derivative | Second derivative

Ramp edge corrupted by steadily increasing amounts of additive Gaussian noise

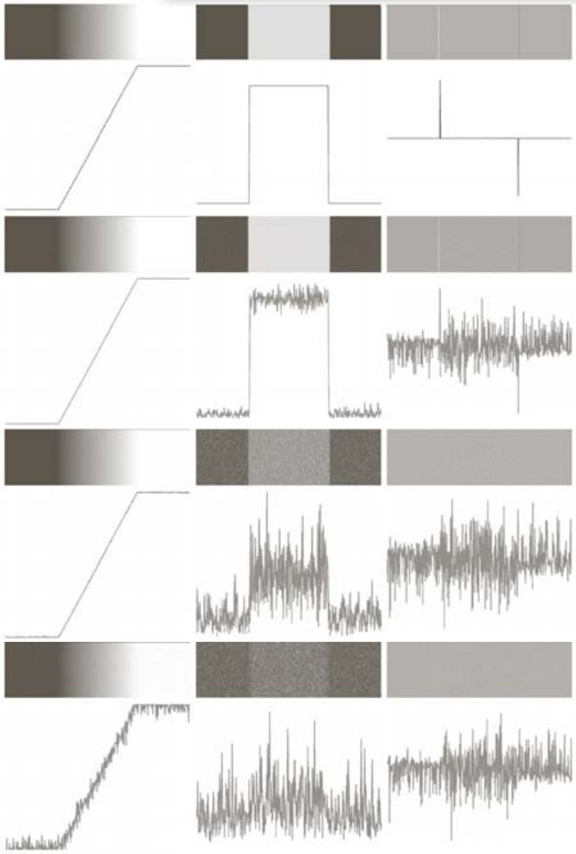

FIGURE 10.11 First column: Images and intensity profiles of a ramp edge corrupted by random Gaussian noise of zero mean and standard deviations of 0.0, 0.1, 1.0, and 10.0 intensity levels, respectively. Second column: First-derivative images and intensity profiles. Third column: Second-derivative images and intensity profiles.

<u>Fundamental steps in edge detection:</u>

1. Smoothing — for noise reduction
2. Detection — of all potential edge candidates
3. Localization — select the real edge points

Line Detection

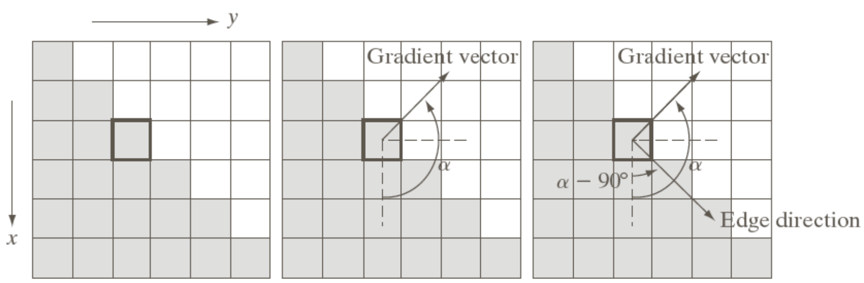

a b c

FIGURE 10.12 Using the gradient to determine edge strength and direction at a point. Note that the edge is perpendicular to the direction of the gradient vector at the point where the gradient is computed. Each square in the figure represents one pixel.

$$\nabla f = \begin{bmatrix} \dfrac{\partial f}{\partial x} \\ \dfrac{\partial f}{\partial y} \end{bmatrix} = \begin{bmatrix} g_x \\ g_y \end{bmatrix}$$

Strength and direction of an edge can be determined using the gradient

Strength (magnitude)

$$M(x,y) = mag(\nabla f) = \sqrt{g_x^2 + g_y^2}$$

Direction

$$\alpha(x,y) = Tan^{-1}\left(\frac{g_x}{g_y}\right)$$

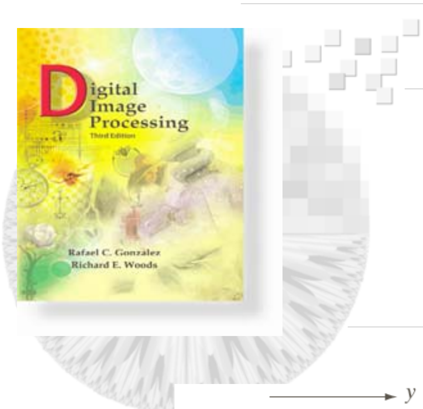

Line Detection

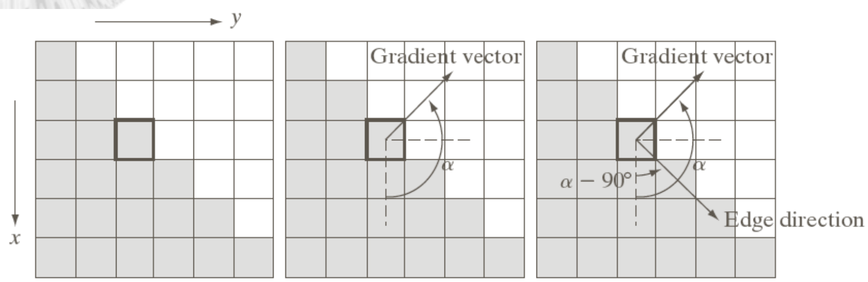

$$\nabla f = \begin{bmatrix} \dfrac{\partial f}{\partial x} \\ \dfrac{\partial f}{\partial y} \end{bmatrix} = \begin{bmatrix} -1 \\ 1 \end{bmatrix}$$

Gray=0, white=1

The gradient vector is perpendicular to the actual edge.

−1
1

−1	1

a b

FIGURE 10.13 One-dimensional masks used to implement Eqs. (10.2-12) and (10.2-13).

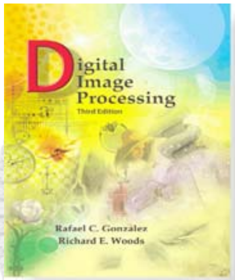

Image Segmentation

z_1	z_2	z_3
z_4	z_5	z_6
z_7	z_8	z_9

−1	0		0	−1
0	1		1	0

Roberts

−1	−1	−1		−1	0	1
0	0	0		−1	0	1
1	1	1		−1	0	1

Prewitt

−1	−2	−1		−1	0	1
0	0	0		−2	0	2
1	2	1		−1	0	1

Sobel

a
b c
d e
f g

FIGURE 10.14 A 3 × 3 region of an image (the z's are intensity values) and various masks used to compute the gradient at the point labeled z_5.

The Prewitt and Sobel are the most commonly used gradient masks

The Sobel has better noise characteristics than the Prewitt

Image Segmentation

Modified Prewitt and Sobel masks for detecting diagonal edges

Prewitt

0	1	1
−1	0	1
−1	−1	0

−1	−1	0
−1	0	1
0	1	1

Sobel

0	1	2
−1	0	1
−2	−1	0

−2	−1	0
−1	0	1
0	1	2

-45°

+45°

a b
c d

FIGURE 10.15 Prewitt and Sobel masks for detecting diagonal edges.

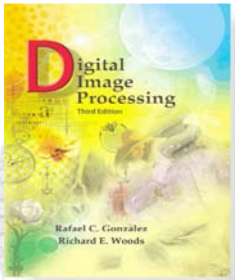

Image Segmentation

1200x1600 original image

$|G_x|$ using 3x3 Sobel

$|G_y|$ using 3x3 Sobel

$|G_x|+|G_y|$ gradient approximation

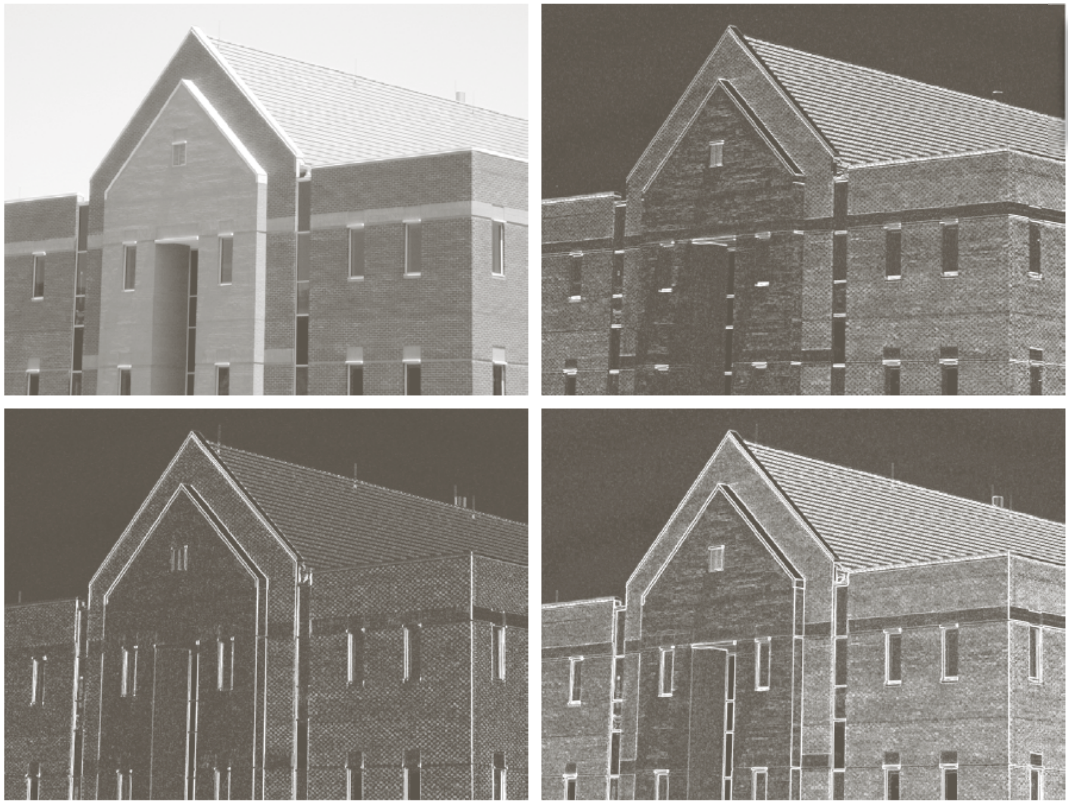

a b
c d

FIGURE 10.16 (a) Original image of size 834×1114 pixels, with intensity values scaled to the range [0, 1]. (b) $|g_x|$, the component of the gradient in the x-direction, obtained using the Sobel mask in Fig. 10.14(f) to filter the image. (c) $|g_y|$, obtained using the mask in Fig. 10.14(g). (d) The gradient image, $|g_x| + |g_y|$.

Image Segmentation

FIGURE 10.17 Gradient angle image computed using Eq. (10.2-11). Areas of constant intensity in this image indicate that the direction of the gradient vector is the same at all the pixel locations in those regions.

Gradient angle plotted as an intensity. Areas of constant intensity have the same gradient vector (perpendicular to the edge). Black means the gradient vector is at 0° so the actual edge is vertical (at -90°)

Image Segmentation

1200x1600 original image smoothed with a 5x5 averaging filter

$|G_x|$ using 3x3 Sobel

$|G_y|$ using 3x3 Sobel

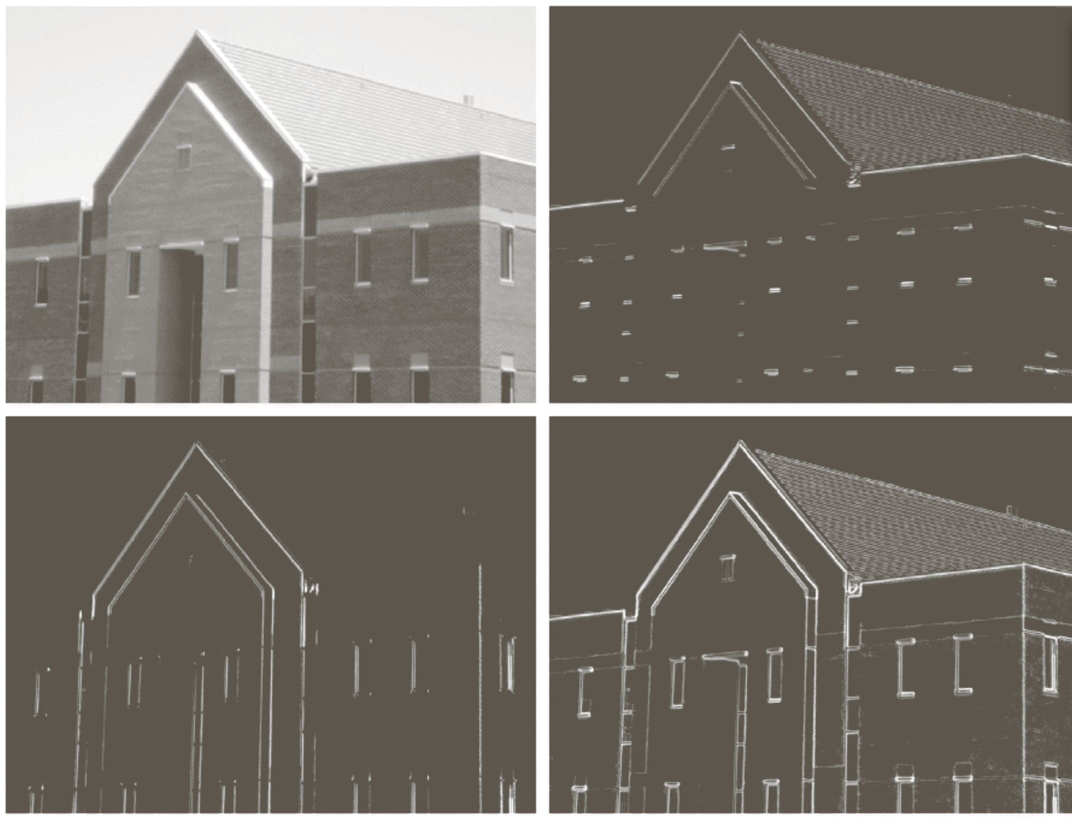

a b
c d

FIGURE 10.18 Same sequence as in Fig. 10.16, but with the original image smoothed using a 5×5 averaging filter prior to edge detection.

$|G_x|+|G_y|$ gradient approximation

Averaging causes the edges to be weaker but cleaner. Note loss of brick edges

Image Segmentation

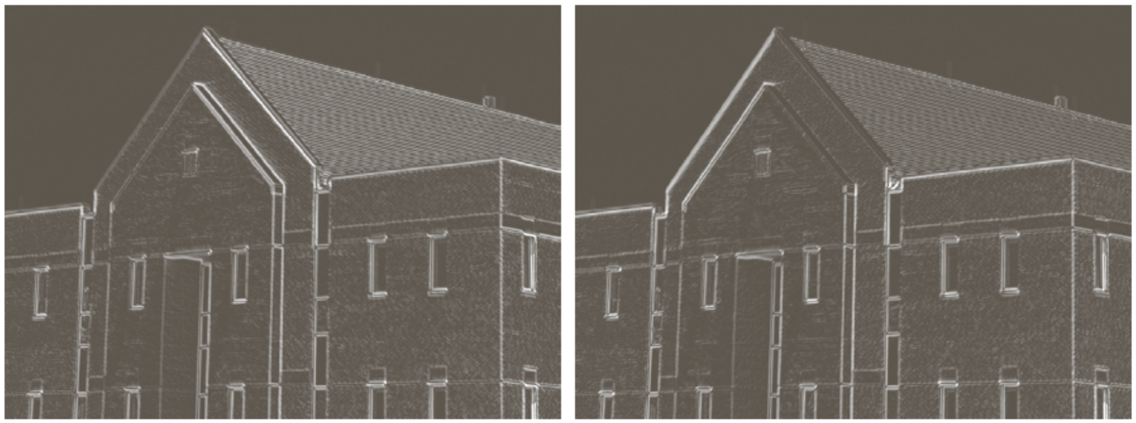

a b

FIGURE 10.19 Diagonal edge detection. (a) Result of using the mask in Fig. 10.15(c). (b) Result of using the mask in Fig. 10.15(d). The input image in both cases was Fig. 10.18(a).

-45° Sobel

+45° Sobel

Note that both can detect a horizontal or vertical edge, but with a weaker response than a horizontal or vertical operator

Image Segmentation

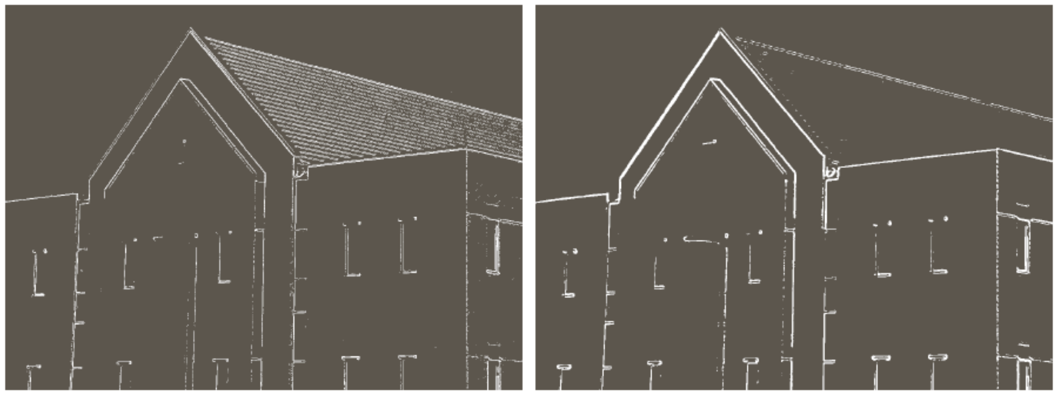

Thresholded gradient image w/o smoothing

Thresholded gradient image w/smoothing

Threshold = 1/3 max_value

a b

FIGURE 10.20 (a) Thresholded version of the image in Fig. 10.16(d), with the threshold selected as 33% of the highest value in the image; this threshold was just high enough to eliminate most of the brick edges in the gradient image. (b) Thresholded version of the image in Fig. 10.18(d), obtained using a threshold equal to 33% of the highest value in that image.

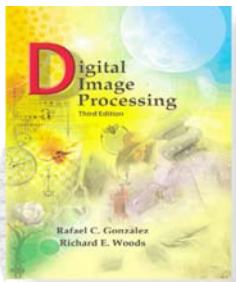

Image Segmentation

The LoG is sometimes called the Mexican hat operator

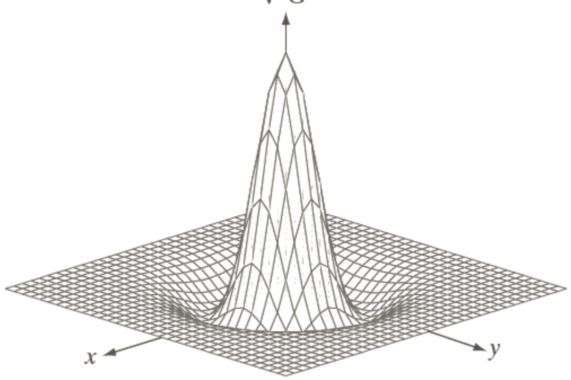

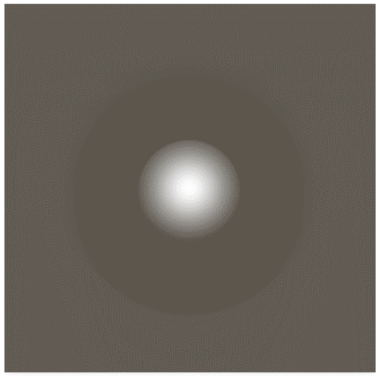

The Laplacian is NEVER used directly because of its strong noise sensitivity

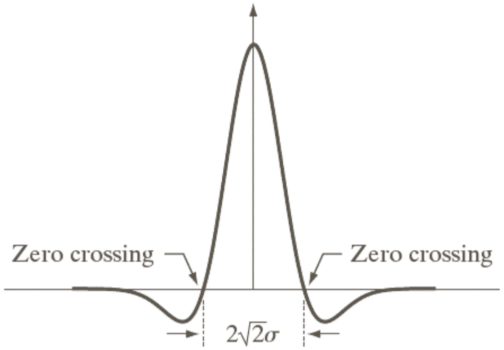

0	0	−1	0	0
0	−1	−2	−1	0
−1	−2	16	−2	−1
0	−1	−2	−1	0
0	0	−1	0	0

a b
c d

FIGURE 10.21 (a) Three-dimensional plot of the *negative* of the LoG. (b) Negative of the LoG displayed as an image. (c) Cross section of (a) showing zero crossings. (d) 5×5 mask approximation to the shape in (a). The negative of this mask would be used in practice.

Combining the Laplacian with a Gaussian gives the LoG

$$\nabla^2 h(r) = -\left[\frac{r^2-\sigma^2}{\sigma^4}\right] e^{-\frac{r^2}{2\sigma^2}}$$

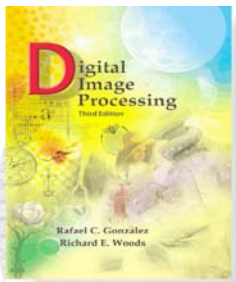

Image Segmentation

Marr-Hildereth algorithm:

- Filter image with a nxn Gaussian low-pass filter $G(x,y) = e^{-\frac{x^2+y^2}{2\sigma^2}}$
- Compute the Laplacian of the filtered image using an appropriate mask
- Find the zero crossings of this image

This operator is based upon a 2nd derivative operator and can be scaled using the parameter σ to fit a particular image or application, i.e., small operators for sharp detail and large operators for blurry edges